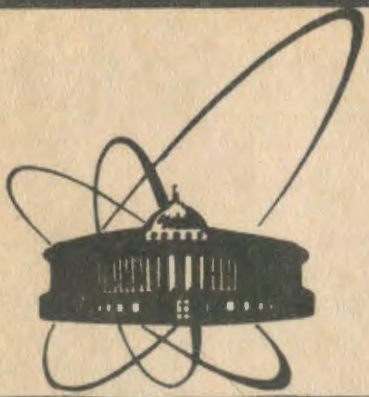

сообщения
объединенного
института
ядерных
исследований
дубна

E4-90-116

M.Gmitro[1], O.Richter[1], H.-R.Kissener[2],
A.A.Ovchinnikova[3]

ORDINARY AND RADIATIVE MUON CAPTURE ON ^{14}N

[1]Permanent address: Institute of Nuclear Physics ČSAV, CS 250 68 Řež (Prague)
[2]Central Institute for Nuclear Research, Rossendorf, GDR
[3]Institute of Nuclear Physics, Moscow State University, Moscow, USSR

1990

1. INTRODUCTION

Both ordinary muon capture (OMC) and radiative muon capture (RMC) involve a sizable momentum transfer and thus appear as appropriate for studying the magnitude of the induced pseudoscalar coupling in the weak hadronic currents. The OMC data are by now available for the majority of possible targets [1]. The observation of RMC, on the contrary, has been very limited: Until recently we have had only data for ^{40}Ca and ^{16}O and low statistic observation for a few heavier nuclei [2]. The use of the time – projection chamber at TRIUMF made by now possible the observation of RMC for a series of nuclei [3]. The extraction of the pseudoscalar coupling constant g_p requires, however, that the photon yield should be theoretically evaluated on the basis of some reliable nuclear response model. Since only inclusive RMC spectra were observed till now, the last task is not easy to meet.

In the present paper we intend to give predictions for the photon spectra due to the RMC reaction on ^{14}N as a prospective target to be used in possible coming experiments. The treatment of the RMC mechanisms closely follows earlier analyses for ^{12}C (Ref.4) and ^{16}O and ^{40}Ca (Ref.5). We shall discuss, however, in detail the peculiarities of the shell model calculations for the A = 14 nuclei. With such information the reader can judge how far the resulting relative photon yield $R = \Lambda_{RMC}/\Lambda_{OMC}$ can be considered as a reliable estimate. The discussion also stresses weak points and shows the ways of improving the calculations.

2. SHELL MODEL STATES

The spin and isospin reduced matrix element of any single particle operator O can be written in the form [6]

$$(E_f J_f T_f \,|||\, \hat{O}_{JT} \,|||\, E_i J_i T_i) = \sum_{a a'} \psi^{fi}_{JT}(a', a)\,(a' \,|||\, \hat{O}_{JT} \,|||\, a)\,. \qquad (1)$$

We have calculated the reduced density matrix elements $\psi^{fi}_{JT}(a', a)$ for A = 14 nuclei in the $(0 + 1)\hbar\omega$ harmonic oscillator basis of the shell model (SM). For the states of normal parity we employed Cohen-Kurath (8-16) 2BME

interaction [7] (in the following CK); for the states of non-normal parity the modified Gillet COP interaction [8] has been adopted. The relevance of this type of effective N-N interaction to the various reactions of interest has been discussed elsewhere [9].

Here we mention only that the spurious contamination has been removed completely from the physical states. The stability of our results against variation of effective N-N interaction has been checked by using also the empirical matrix elements fitted by van Hees [10]. We have found that the total transition rates are fairly independent of the SM option for the N-N interaction.

The low-lying states of non-normal parity in A = 14 nuclei are all accounted for and quite well reproduced within the frame of the $1\hbar\omega$ model space (see also Ref. [10]). Much less satisfactory is the description obtained within the $0\hbar\omega$ space for the natural parity levels. In the remaining part of this Section we discuss the related problems.

2.1. The $0\hbar\omega$ Model Space and A = 14 Nuclei

The SM $0\hbar\omega$ basis for mass number A = 14, isospin T = 1, provides only two $J=0^+$ and two $J=2^+$ states. So it is clear, the $0\hbar\omega$ basis is too poor to describe all the experimentally known low-lying normal parity states in ^{14}C. Due to the well pronounced configurational splitting between Young tableaux [442] and [433], the upper and lower $J=0^+$ and $J=2^+$ $0\hbar\omega$ states are separated as much as by 8-10 MeV for both interactions used by us. As a consequence, the experimentally known ^{14}C states 0_2^+, 0_3^+, 2_2^+, 2_3^+ have to be interpreted as intruder states in $0\hbar\omega$. The two lowest 2^+ (at 7.01 and 8.32 MeV) lie so close to each other, that probably, they both contain a strong mixture of $0\hbar\omega$ and $2\hbar\omega$ configurations. Actually, S.Lie [11] restricting the space to the 2sd active particles, revealed a sizable admixture of $p^{-2}(2sd)^2$ configurations in some low-lying A = 14 states, and namely as large as about 50% in both 2_1^+1 and 2_2^+1 states. On the other hand, the ground states of ^{14}N and ^{14}C contain only a negligible $2\hbar\omega$ admixture. Lie succeeded to reduce twice the electromagnetic M1 transition strength to the 2_1^+1 state (in ^{14}N), overestimated by the factor of 4 in $0\hbar\omega$ calculations. The summed transition strength to the 2_1^+1 and 2_2^+1 states remains, however, almost the same as the one calculated in $0\hbar\omega$ space for 2_1^+1 state. The transition strength is only redistributed or spread to the $0\hbar\omega$ components of Lie's 2_1^+1 and 2_2^+1 states. In other words, a portion of the transition strength to the 2_2^+1 state is already contained in the transition to the 2_1^+1 state, if calculated in $0\hbar\omega$ space. It should be stressed, however, that this summed transition strength is indeed too high, by a factor of 2, when compared with experimental data [12]. Similar overestimation by a factor of 2 of the summed transition strength, we discuss, is observed in radiative pion capture (RPC) [13-15]. This puzzle cannot be solved

by adding $p^{-2}(2sd)^2$ configurations to the $0h\omega$ space only, but rather requires a full $0h\omega + 2h\omega$ space calculation. The recent measurement of angular distributions in $^{14}N(\gamma, \pi^+)^{14}C^*$ (Ref.[16]) even shows that the restriction on $p^{-2}(2sd)^2$ excitations results in still further disagreement between theory and experiment.

It has been argued long ago[17], that the large $p^{-1}(3pf)$ admixtures as low as 11 MeV in ^{14}N might play an important role. Recently, the Utrecht group[18] has found 20% of $p^{-1}(3pf)$ and 10% of $p^{-2}(2sd)^2$ configurations even in the ground states of A = 14 and A = 15 nuclei, using the full $0h\omega + 2h\omega$ model space. Although in the experiment[19] on $^{15}N(\vec{d}, t)^{14}N$ no significant $\ell = 2$ and/or $\ell = 3$ pickup would be identified, it was not possible to disentangle the 1p and 3p contributions to the $\ell = 1$ transitions. Because some discrepancies between T = 1 CK matrix elements and those estimated from experiment have been found, it could be a result of just the 3p configurations interplay. Such admixtures would change the one-particle transition strength calculated, and namely in the $2^+_1 1$ and $2^+_2 1$ states. Unfortunately, we were not able to investigate this problem properly, due to the technical complications.

At the end of this section we would like to mention a selection rule that governs M1 transitions in the $0h\omega$ space and explains why the $2^+ 1$ states exhaust a good deal of M1 strength in A = 14 nuclei.

In the limit of LS classification of nuclear states, for the matrix element of the transition operator $\hat{O}$ one has

$$([f_f] L_f S_f J_f \,||| \hat{O}_{LSJ} ||| [f_i] L_i S_i J_i) = \begin{Bmatrix} L_i & S_i & J_i \\ L & S & J \\ L_f & S_f & J_f \end{Bmatrix} C([f_f],[f_i]), \quad (2)$$

where the expression C involves the product of coefficients of fractional parentage and the single-particle matrix elements. The Young tableaux [f] classify the spatial symmetry of nuclear wave functions. The 9j-symbol expresses selection rules for angular momenta. It can be proved that due to the relative simplicity of the $0h\omega$ space, one obtains

$$C([f_f],[f_i]) \sim \delta([f_f],[f_i]) \quad \text{if} \quad L = 0. \quad (3)$$

In the wave function of ^{14}N ground state, there is a strongly dominating component [442] ^{13}D, with the weight $a^2 \approx 0.9$ fairly independent of the effective N-N interaction used. In the ground state wave function of ^{14}C there is neither the D component nor the symmetry [442] dominates. Therefore the ground state L = 0, M1 transitions are hindered, and the strength is distributed in the other excited states. The $2^+_1 1$ level of ^{14}C ($E_x = 7.01$ MeV)

contains a large $[442]^{31}D_2$ component. And namely this component, even spread if the model space is enlarged, does contribute to the M1 sum rules. This enhancement of the M1 transition to the low-lying 2^+1 states (7.01 and 8.32 MeV or ^{14}N analogs) was observed in RPC, /13,15/ electron scattering /20/, photoproduction of pions /16/ as well as in OMC /21/.

3. MUON CAPTURE

In the case of RMC reaction, the transition operator $\hat{O}$ has the form /5/

$$\hat{O}_{J1} = \begin{pmatrix} \ell & \ell' & L \\ 0 & 0 & 0 \end{pmatrix} j_\ell(kr)\, j_{\ell'}(nr)\, [\, Y_L(\hat{r}) \otimes \sigma_S \,]_J\, \tau^{(-)}. \qquad (4)$$

Here σ_S for S = 0 (S = 1) is the unit (Pauli) matrix, $\tau^{(-)}$ is the isospin lowering operator, k and n are photon and neutrino energies, respectively. The spherical Bessel function $j_{\ell'}(nr)$ stems from the partial wave decomposition of the outgoing neutrino and $j_\ell(kr)$ from the decomposition of the photon plane waves. The necessity to expand outgoing neutrino and photon waves separately is a technical consequence of the modified impulse approximation (MIA) /5/ based essentially on the continuity equation for nuclear electromagnetic current. This technique helps to include partly the meson exchange current corrections /2/. The relation between impulse approximation and MIA can be found in /2,5/.

The transition operator for OMC can be obtained from Eq.(4) in the limit of $k \to 0$, $\ell = 0$. In this case, the operator $\hat{O}$ in Eq.(4) contains only one spherical Bessel function, of the argument qr, where q = n is the transferred momentum limited by the muon mass as $q \leq 0.5\ fm^{-1}$. The higher partial waves L in Eq.(4) are effectively suppressed in radial integrals because they are evaluated within the nuclear volume ($qR < 2$). In RMC, due to the richer structure of the transition operator O in Eq.(4) (two spherical Bessel functions), the L = 2 partial wave is less suppressed as compared to OMC. This influences M1 transitions through the operator $[\, Y_2 \otimes \sigma \,]_{1^+}$.

Due to the computer limitations, we have omitted velocity-dependent operators like $[\, Y_L \otimes \nabla \,]_J$. It was demonstrated /22/ that although one loses about 10% of the capture rate, the ratio of RMC to OMC rates is only negligibly changed when the velocity dependent operators are consistently omitted in both rate calculations.

4. THE OBSERVED QUANTITIES

Starting with the effective RMC Hamiltonian one derives the full RMC amplitude $M(\rho)$ see Ref. /5/. Summing over the polarization and integrating over all directions of the outgoing neutrino momentum, the exclusive photon spectrum corresponding to the transition from the state $|E_i J_i M_i>$ to the state $|E_f J_f M_f>$ is given as

$$N^{fi}(k) = \frac{2(\alpha Z)^3}{(2\pi)^4 h} \alpha (G \cos\theta_C)^2 \, m_\mu \, C(Z) \times$$
$$\times k (k^{fi}_{max} - k)^2 \, \frac{1}{2(2J_i + 1)} \sum_{\rho M_i M_f} |M(\rho)|^2 . \qquad (5)$$

Here α and G are the electromagnetic and weak interaction constants, θ_C is the Cabbibo angle and C(Z) stems from the muon atomic wave function; ρ is the polarization index of the outgoing photon and k^{fi}_{max} is the maximum photon energy. Performing the integration over the photon energy k, we obtain the partial RMC rate

$$\Lambda^{fi}_{RMC} = \int N^{fi}(k) \, dk . \qquad (6)$$

The inclusive energy photon spectrum is obtained from Eq.(5) by summing over all final nuclear states

$$N(k) = \sum_f N^{fi}(k) . \qquad (7)$$

The total RMC rate is the integral of N(k) over the photon energy

$$\Lambda_{RMC} = \int N(k) \, dk . \qquad (8)$$

The OMC amplitude M can be derived from that of RMC using the limit $k \to 0$. The OMC rate is then given as

$$\Lambda_{OMC} = \frac{2}{\pi h} (nG \cos\theta_C)^2 \, (m_\mu \alpha Z)^3 \, C(Z) \, \frac{1}{2(2J_i + 1)} \sum_{M_i M_f} |M|^2 . \qquad (9)$$

The quantities most frequently quoted for RMC are the relative photon spectrum

$$R(k) = \frac{N(k)}{\Lambda_{OMC}}, \tag{10}$$

and the branching ratio

$$R = \frac{\Lambda_{RMC}}{\Lambda_{OMC}}. \tag{11}$$

5. RESULTS

A. Ordinary Muon Capture

In table 1 we show the dependence of the OMC rate on the induced pseudoscalar coupling constant g_P (the axial vector coupling constant $g_A = -1.24$), and the contributions of positive- and negative-parity states separately. The OMC rate depends moderately on g_P, it varies by about 17% for the values of g_P/g_A between 4.5 and 20. The canonical value of g_P derived as a PCAC prediction is $g_P/g_A = 6.78$ (see, e.g., Ref. [2]). However, in the SM calculations for the ^{12}C target [4, 23], one apparently needs an enhanced pseudoscalar coupling constant g_P/g_A in order to reproduce the data. The experimental value [1] of the OMC rate on ^{14}N, $\Lambda^{exp}_{OMC} = (69300 \pm 800)\ s^{-1}$ is lower in comparison with that we have calculated. As is discussed above, however, it is clear that the $0\hbar\omega$ configuration space is too poor to ensure a realistic description of the absolute capture rate Λ_{OMC}.

In table 2 we have selected some partial transitions giving main contributions ($\Lambda^{fi}_{OMC} > 2000\ s^{-1}$) to the total rate. The dominance of selected states is not significantly influenced by the value g_P used for calculations, so we have chosen as a representative one the value $g_P/g_A = 16$. As concerns the experiment, there was measured [21] the partial transition rate to the $2^+_1 1$

Table 1. OMC rates in s^{-1} summed over the positive (Λ^+_{OMC}) and negative (Λ^-_{OMC}) parity states in ^{14}C and total OMC rates in dependence on g_P

g_P/g_A	4.5	7.5	10	12	14	16	20
Λ^+_{OMC}	29450	27870	26810	26130	25600	25220	24910
Λ^-_{OMC}	71870	68060	65430	63660	62200	61050	59670
Λ_{OMC}	101320	95930	92240	89790	87800	86270	84590

Table 2. OMC rates for several dominant partial transitions calculated with $g_P/g_A = 16$

$E_x(^{14}C, MeV)$	$J_f^\pi T$	$\Lambda_{OMC}^{fi}(s^{-1})$	Dominant multipolarity
7.0	2^+1	22750	M1, E2
11.3	1^+1	2010	E2, M1
6.7	3^-1	3060	M2, E3
14.9	3^-1	3380	M2
15.7	3^-1	2540	M2
14.6	2^-1	2530	M2
17.8	2^-1	2240	M2
18.4	2^-1	5830	E1

state at $E_x = 7.01$ MeV, with the result $\Lambda_{OMC}(2^+) = (4640 \pm 700)\ s^{-1}$. This experimental value is by about a factor of 4 lower than our estimate. The same overestimate was obtained also in other calculations [24,25]. We have discussed the source of this discrepancy in section 2.1. Following the arguments given there, we estimate that our results for $\Lambda_{OMC}(2^+)$ would also be twice as large as the summed 2^+1 transition rate, if it were measured. So, we should reduce our calculated total OMC rate by $\Delta\Lambda_{OMC} \approx 12000\ s^{-1}$ independently of the magnitude of the pseudoscalar coupling. Thus, the corrected total OMC rate is $\Lambda_{OMC}(g_P/g_A = 16) = 74000\ s^{-1}$. One should realize, however, that this result will be increased by about 10% if the nucleon-velocity dependent terms omitted here (cf.Sect.3) are included into the calculation.

Among other major contributions to the total OMC rate, we have obtained the strong excitation of the 1_1^+1 state at $E_x = 11.3$ MeV. Analogous strength was seen in RPC [13,15] at 10-13 MeV. We predict also a strong excitation of the 3^-1 state at $E_x = 6.7$ MeV. Some indication of this level was found in the OMC data [26]. The GDR region built on the ^{14}N has been studied through photoexcitation and radiative proton capture. The $^{13}C(p,\gamma)^{14}N^*$ excitation function [27] shows a broad structure in the region $18 \le E_x \le 24$ MeV with prominent peaks at $E_x = 22.5$ and 23.0 MeV. The analogs in ^{14}C are expected at $E_x \approx 20$ MeV. Much of this strength is associated with 2^-1 states. Our calculations provide a strong E1 transition to the 2^-1 state placed by the Gillet COP force by 2 MeV low. The M2 transitions to the states 2^-1 and 3^-1 predicted just below the main peak in the GDR region could be probably connected to the broad structure in the photon spectrum which has been observed in RPC [15] near $E_x \approx 15$ BMeV. These transitions constitute the spin-isospin dipole vibrations.

B. Radiative Muon Capture

In table 3 we present the partial RMC rates summed over all nuclear final states with the definite spin and parity $\Lambda_{RMC}(J^{\pi})$, the total RMC rate Λ_{RMC}, and the branching ratio R. In the energy integration only the interval $k \geq 57$ MeV is taken into account; below this energy the RMC photons cannot be observed due to the μ-decay bremsstrahlung background. We have also calculated the relative photon spectra R(k) as a functions of g_P/g_A, they are presented in Table 4.

There are always only a few nuclear states which provide major contributions to the total reactions probability and these states are the same for both OMC and RMC. (The only exception is the transition $^{14}N_{g.s.} \rightarrow {}^{14}C_{g.s.}$ discussed in Sect.3). It is therefore a reasonable approximation to take for the calculation of R a subset of the shell model states most strongly excited in the OMC. Namely we have limited the summation for both OMC and RMC by those states which show up $\Lambda_{OMC}(\text{partial}) \geq 100\ s^{-1}$. They exhaust about 96% of the calculated total OMC rate.

As we have expected, the calculated partial rate to the $2^+_1 1$ state is very high. As in the OMC reaction, we suppose that this rate is overestimated by a factor of 2. Taking this into account, we should reduce the total RMC rate for $g_P/g_A = 16$ by $\Delta\Lambda_{RMC} = 0.290\ s^{-1}$. Remembering the similar reduction in the OMC reaction ($\Delta\Lambda_{OMC} = 12000\ s^{-1}$), we can evaluate the corrected branching ratio $\bar{R}(g_P/g_A = 16) = 1.91/74270 = 2.57 \times 10^{-5}$. This corrected value does not differ significantly from the uncorrected one presented in

Table 3. RMC rates (in s^{-1}) summed over the nuclear final states of a given spin and parity J^{π}, total RMC rates, and the branching ratio R (in 10^{-5}) in dependence on g_P

g_P/g_A	7.5	10	12	14	16	20
Λ_{RMC} (0^+)	0.041	0.048	0.055	0.064	0.076	0.103
Λ_{RMC} (1^+)	0.051	0.050	0.049	0.049	0.049	0.052
Λ_{RMC} (2^+)	0.708	0.658	0.627	0.603	0.589	0.578
Λ_{RMC} (0^-)	0.048	0.057	0.066	0.074	0.086	0.112
Λ_{RMC} (1^-)	0.231	0.251	0.272	0.299	0.329	0.402
Λ_{RMC} (2^-)	0.430	0.485	0.538	0.560	0.669	0.833
Λ_{RMC} (3^-)	0.328	0.339	0.354	0.374	0.400	0.468
Λ_{RMC}	1.825	1.888	1.963	2.064	2.199	2.550
R	1.90	2.05	2.19	2.39	2.55	3.01

Table 4. Relative spectrum $R(k) = N(k)/\Lambda_{OMC}$ (in 10^{-6} MeV^{-1}) as a function of the photon energy

k(MeV)	g_P/g_A=7.5	10	12	14	16	20
57	1.28	1.34	1.39	1.46	1.55	1.75
64	0.98	1.05	1.11	1.19	1.28	1.50
71	0.64	0.70	0.75	0.82	0.89	1.08
78	0.32	0.35	0.38	0.42	0.46	0.56
85	0.11	0.12	0.13	0.14	0.16	0.20

table 3. The same holds also for other pseudoscalar coupling. We believe therefore that the calculated branching ratios R are not significantly distorted by the unsufficient size of the $0\hbar\omega$ space discussed in Sect.2.1.

The earlier calculation of the RMC rates on ^{12}C (Ref.[4]) has shown a good agreement with the data ($R = (2.3 \pm 0.2) \times 10^{-5}$) of Ref.[28] if an enhanced value of the pseudoscalar coupling, $g_P/g_A \approx 16$, has been used. For ^{16}O two groups of data are available. The measurements by Döbeli et al.[29] ($R = (2.44 \pm 0.47) \times 10^{-5}$) and Armstrong et al.[30] ($R = (2.2 \pm 0.2) \times 10^{-5}$), if combined with the calculations of Ref.[5], also lead to a preference of the anhanced value of $g_P/g_A \gtrsim 14$. The measurement by Frischknecht et al.[31] on ^{16}O ($R = (3.8 \pm 0.4) \times 10^{-5}$) indicates an even much larger value of g_P, $g_P/g_A > 20$. It is therefore highly interesting to have data for other targets, for the ^{14}N considered here in particular.

6. CONCLUSIONS

Both OMC and RMC reactions selectively excite the analogs of giant M1 states of the target. The $0\hbar\omega$ shell model space does not suffice for the proper description of all experimentally known normal parity levels of A = 14 nuclei. This concerns, particularly, strongly excited states 2^+1 at the ^{14}C excitation energy 7.01 and 8.32 MeV. For the correct description of these levels it is not enough to include only $p^{-2}(2sd)^2$ configurations but a full $0\hbar\omega + 2\hbar\omega$ calculation is needed. Especially the influence of $p^{-1}(3pf)$ configurations for the nuclei near the upper end of the p-shell should be investigated carefully. The inability of $0\hbar\omega$ calculation to treat properly all positive parity states in ^{14}N and ^{14}C does not influence significantly the value of the branching ratio R for RMC. The negative parity states of A = 14 nuclei are, in general, well described in the frame of $1\hbar\omega$ space. The calculations give evidence for

excitations of spin-isospin dipole vibrations in the GDR region. The predominant contributions are from 2^- and 3^- states. The RMC branching ratio R is a sensitive function of induced pseudoscalar coupling constant g_p. The measurement of RMC on the ^{14}N target is desirable.

REFERENCES

1. Suzuki T., Measday D.F., Roalsvig J.P. — Phys.Rev., 1987, C35, p.2212.
2. Gmitro M., Truöl P. — In: Adv. in Nucl.Phys., ed. J.W.Negele and E.Vogt, (Plenum, New York, 1987), vol.18, p.241.
3. Hasinoff M.D. et al. — TRIUMF report TRI-PP-89-54, June, 1989.
4. Gmitro M. et al. — Nucl.Phys. in press.
5. Gmitro M., Ovchinnikova A.A., Tetereva T.V. — Nucl.Phys., 1986, A453, p.685.
6. Tiator L., Wright L.E. — Phys.Rev., 1984, C30, p.989.
7. Cohen S., Kurath D. — Nucl.Phys., 1965, 73, p.1.
8. Jäger H.U., Kirchbach M. — Nucl.Phys., 1977, A291, p.52.
9. Gmitro M. et al. — Sov.J.Part.Nuclei, 1983, 14, p.323.
10. A.G.M. van Hees, P.W.M.Glaudemans — Z.Phys., 1983, A314, p.323; 1984, A315,p.223.
11. Lie S. — Nucl.Phys., 1972, A181, p.517.
12. Ajzenberg-Selove F. — Nucl.Phys., 1986, A449, p.1.
13. Baer H.W. et al. — Phys.Rev., 1975, C12, p.921.
14. Kissener H.R. et al. — Nucl.Phys., 1978, A302, p.523.
15. Perroud J.P. et al. — Nucl.Phys., 1986, A453, p.542.
16. Sung B.N. et al. — Nucl.Phys., 1987, A473, p.705.
17. Mangelson N.F., Harvey B.G., Glendenning N.K. — Nucl.Phys., 1968, A117, p.161.
18. Wolters A.A., A.G.M. van Hees, Glaudemans P.W.M. — Europhys.Lett., 1988, 5, p.7; Poppellier N.A.F.M., Wood L.D., Glaudemans P.W.M. — Phys.Lett., 1985, 157B, p.120.
19. Saha S.K. et al. — Phys.Rev., 1989, C40, p.39.
20. Clerc H.-G., Kuphal E. — Z.Phys., 1968, 211, p.452.
21. Giffon M. et al. — Phys.Rev., 1981, C24, p.241.
22. Gmitro M. et al. — Czech.J.Phys., 1981, B31, p.499.
23. Ohtsuka N. — Nucl.Phys., 1981, A370, p.431.
24. Mukhopadhyay N.C. — Phys.Lett., 1973, 44B, p.33.
25. Desgolard P., Guichon P.A.M. — Phys.Rev., 1979, C19, p.120.
26. Belloti E. et al. — SIN Physics Report, 1976, 1, p.41.
27. Riess F., O'Connel U.J., Paul P. — Nucl.Phys., 1971, A175, p.462.
28. Armstrong D.S. — Thesis, Univ. of Brit. Columbia, October 1988.
29. Dõbeli M. et al. — Phys.Rev., 1988, C37, p.1633.
30. Armstrong D.S. et al. — TRIUMF preprint TRI-PP-89-2.
31. Frischknecht A. et al. — Phys.Rev., 1988, C38, p.1996.

Received by Publishing Department
on February 19, 1989.